Importance of Correlation Effects in hcp Iron Revealed by a Pressure-Induced Electronic Topological Transition

K. Glazyrin, L. V. Pourovskii, L. Dubrovinsky, O. Narygina, C. McCammon, B. Hewener, V. Schünemann, J. Wolny, K. Muffler, A. I. Chumakov, W. Crichton, M. Hanfland, V. B. Prakapenka, F. Tasnádi, M. Ekholm, M. Aichhorn, V. Vildosola, A. V. Ruban, M. I. Katsnelson, and I. A. Abrikosov

Phys. Rev. Lett. **110**, 117206 — Published 12 March 2013

DOI: 10.1103/PhysRevLett.110.117206

Importance of correlation effects in hcp iron revealed by a pressure-induced electronic topological transition

K. Glazyrin[1,2], L.V. Pourovskii[3,4], L. Dubrovinsky[1], O. Narygina[5], C. McCammon[1], B. Hewener[6], V. Schünemann[6], J. Wolny[6], K. Muffler[6], A. I. Chumakov[7], W. Crichton[7], M. Hanfland[7], V. Prakapenka[8], F. Tasnádi[9], M. Ekholm[3], M. Aichhorn[10], V. Vildosola[11], A. V. Ruban[12], M. I. Katsnelson[13], I. A. Abrikosov[9]

[1] *Bayerisches Geoinstitut, Universität Bayreuth, 95440 Bayreuth, Germany,*
[2] *Yale University, 06511 New Haven, CT, USA*
[3] *Swedish e-science Research Center (SeRC), Department of Physics, Chemistry and Biology (IFM), Linköping University, Linköping, Sweden*
[4¶] *Center de Physique Theorique, Ecole Polytechnique, 91128 Palaiseau Cedex, France*
[5] *School of Physics and Astronomy, University of Edinburgh, Edinburgh, UK*
[6] *Technische Universität Kaiserslautern, Kaiserslautern, Germany*
[7] *ESRF, F-38043 Grenoble Cedex, France*
[8] *GeoSoilEnviroCARS, University of Chicago, Argonne National Laboratory, Argonne, IL 60439, USA*
[9] *Department of Physics, Chemistry and Biology (IFM), Linköping University, Linköping, Sweden*
[10] *Institute of theoretical and computational physics, TU Graz, 8010 Graz, Austria*
[11] *Centro Atómico Constituyentes, GIyANN, CNEA, San Martin, Buenos Aires, Comisión Nacional de Investigaciones Científicas y Técnicas, Ciudad de Buenos Aires, Argentina*
[12] *Department of Materials Science and Engineering, Royal Institute of Technology, SE-10044, Stockholm, Sweden*
[13] *Radboud University Nijmegen, Institute for Molecules and Materials, 6525 AJ, Nijmegen, Netherlands*

Abstract

We discover that *hcp* phases of Fe and $Fe_{0.9}Ni_{0.1}$ undergo an electronic topological transition at pressures of about 40 GPa. This topological change of the Fermi surface manifests itself through anomalous behavior of the Debye sound velocity, *c/a* lattice parameter ratio and Mössbauer center shift observed in our experiments. First-principles simulations within the dynamic mean field approach demonstrate that the transition is induced by many-electron effects. It is absent in one-electron calculations and represents a clear signature of correlation effects in *hcp* Fe.

Iron is the most abundant element on our planet. It is one of the most important technological materials and, at the same time, one of the most challenging elements for the modern theory. As a consequence, the study of iron and iron-based alloys has been a focus of experimental and computational research over the past decades. Recently, investigations of phase relations and physical properties of iron and its alloys at high pressure led to new exciting discoveries including evidence for a body-centred-cubic (*bcc*) phase of iron-nickel alloy at conditions of the Earth's core [1]and the observation of superconductivity in the high-pressure hexagonal close packed (*hcp*) phase of iron in the pressure range 15-30 GPa and at temperatures below 2 K [2].

While the structural properties of iron and iron-nickel alloys at pressures below 100 GPa are well established [3], their electronic and magnetic properties are still debated. The α-phases (*bcc*) of Fe and $Fe_{0.9}Ni_{0.1}$ are ferromagnetic at ambient conditions, but an accurate description of the electronic structure of α-Fe and its high-temperature magnetism require a proper treatment of the many-electron effects [4,5]. The γ-phases (face-centered cubic, *fcc*) are believed to have complex incommensurate magnetic ground states [6], which are still not reproduced by theory [7]**.** The importance of correlation effects for the description of the α- to γ-phase transition in Fe at elevated temperature and ambient pressure has been recently underlined [8]. The ε-phases (*hcp*) of Fe and $Fe_{0.9}Ni_{0.1}$ were previously believed to be nonmagnetic [9]; however recent theoretical work showed that a collinear antiferromagnetic state (AFM-II) [10–12]or a more complex AFM

state [13] have lower energy than the nonmagnetic state. Nevertheless, the AFM-II phase could not be resolved in Mössbauer experiments. Moreover, theoretical estimates of the Néel temperature T_N yield a maximum value of ~69 K for *hcp* Fe at the transition pressure (12 GPa), followed by a decrease with increasing pressure [14]. Although nickel atoms are predicted to enhance the magnetic moments on neighboring iron atoms, there is no evidence that ε-$Fe_{0.9}Ni_{0.1}$ is a static antiferromagnet down to at least 11 K at 21 GPa [12], implying that direct comparison is unreliable between static (0 K) *ab initio* calculations for AFM ε-Fe and room temperature experimental data that clearly indicate a paramagnetic phase. It is worth noting that *hcp* Fe becomes superconducting in the same pressure range [2], and that the mechanism of superconductivity is believed to be unconventional [15]. These observations indicate that the physical behavior of *hcp* Fe at moderate pressures below 70 GPa is complex and the role of correlation effects beyond the standard density-functional (DFT) approach in the physics of this material is not well understood.

In order to unravel the evolution of the electronic structure in *hcp* Fe and $Fe_{0.9}Ni_{0.1}$ under pressure we have carried out a combined experimental and theoretical investigation. We have extracted the Debye sound velocity V_D for pure Fe and $Fe_{0.9}Ni_{0.1}$ alloy from nuclear inelastic scattering (NIS) experiments as well as precisely measured the lattice parameter *c/a* ratio and the Mössbauer centre shift in the pressure range from 12 to 70 GPa. The diamond anvil cell high pressure experiments were conducted out at ESRF beamlines ID09a (X-ray diffraction), ID18 (nuclear resonant inelastic X-ray scattering) and Bayerisches Geoinstitut (Mössbauer spectroscopy). Technical details are given in Supplementary Information [16].

All of our results show anomalous behavior at a similar pressure ~ 40 GPa. Our state-of–the-art *ab initio* simulations within the dynamical mean-field theory [17–19] reveal an electronic topological transition (ETT) in the *hcp* phase of iron at pressures of about 30-40 GPa, providing an explanation of the experimentally observed anomalies. The absence of the ETT in conventional one-electron DFT calculations demonstrates that many-body correlation effects determine the Fermi surface topology of paramagnetic *hcp* Fe, and, therefore, essential for the correct description of the complex physical phenomena observed in this material.

Figure 1 summarizes our experimental measurements of the Debye sound velocity V_D for Fe and $Fe_{0.9}Ni_{0.1}$ extracted from NIS experiments. The experimental data show a softening of V_D in the pressure range 42-52 GPa. To verify our results we also analyzed the available literature [20–23]and conclude that the same softening of V_D has been observed at pressures of 40-50 GPa. The phenomenon was not given much attention in the previous publications, perhaps due to data scatter and the uncertainties of individual data points.

The softening of the Debye sound velocity in Fig. 1 is weak, so we made further investigations. We measured the lattice parameters of *hcp*-Fe in a diamond anvil cell (DAC) on compression to ~65 GPa in quasi-hydrostatic He pressure transmitting medium at ambient temperature and found an anomaly in *c/a* at about 40 GPa (Fig. 2a), consistent with the pressure at which V_D shows softening. The pressure dependence of the *c/a* ratio in *hcp* Fe has been the subject of several previous experimental studies [24–29]that were mainly focused on much higher pressures. However, a closer inspection of the Dewaele *et al.* results [26] shows a very good agreement with our data (*Fig. S.1.3* [16]). Also, an anomalous behavior of *c/a* was reported at about 50 GPa based on a limited number of data points collected in DAC experiments using a non-hydrostatic (NaCl) pressure-transmitting medium [29].

Mössbauer spectroscopy can also be a powerful method to detect pressure-induced transitions [30]. We performed Mössbauer experiments on pure Fe and $Fe_{0.9}Ni_{0.1}$ up to 60 GPa in a DAC loaded with He as a quasi-hydrostatic pressure transmitting medium, and observed a large anomaly in the center shift variation with pressure at 40-45 GPa (Fig. 2b). Our theoretical calculations demonstrate that the anomaly cannot be explained by changes of the electron density at the nuclei and, correspondingly, of the isomer shift [16]. Therefore, the anomaly must be associated with the second-order Doppler shift [30].

We have shown from three independent experimental methods pressure-induced anomalies in the pressure range 40-50 GPa. We note that X-ray diffraction does not reveal any crystallographic structural change of *hcp*-Fe and $Fe_{0.9}Ni_{0.1}$ at the same conditions [1,31,32], and as discussed above, there is no long range magnetic order in the *hcp* phase of Fe detected by experiments. The observed anomalies must therefore be

associated with changes in the electronic state of paramagnetic *hcp*-Fe and $Fe_{0.9}Ni_{0.1}$. To address this question we made a theoretical investigation of the electronic structure of ε-Fe at moderate pressures in the range 12-70 GPa. We employed a state-of-the-art fully self-consistent technique [19] combining full-potential linearized augmented plain-wave (LAPW) band structure method with the dynamical mean-field theory (DMFT) treatment of the on-site Coulomb repulsion between Fe 3*d* states [16]. The DMFT quantum impurity problem was solved using the exact Continuous-time strong-coupling Quantum Monte-Carlo method [33]. A combination of LDA and DMFT has been applied previously to investigate thermodynamic stability [8] and to describe the magnetic properties [4] of paramagnetic *bcc* Fe at ambient pressure, which justifies the choice of method for this work. Our LDA+DMFT simulations predict a paramagnetic phase for *hcp* Fe at room temperature (see Sec. 2.5 of Supplementary [16]), in agreement with experimental observations.

The LDA+DMFT Fermi surfaces and ***k***-resolved spectral functions for two different volumes are shown in Fig. 3. The *hcp* phase of Fe is predicted to be weakly correlated, with the average mass enhancement decreasing from 1.43 at 16 GPa to 1.25 at 69 GPa, indicating a reduced correlation strength at smaller volumes. Sharp bands in the vicinity of the Fermi level ε_F and a noticeable shift of bands toward ε_F compared to the LDA picture (Fig. 3 (e) and (f)) are the usual features of a Fermi liquid. Most interestingly, the hole-like bands at the **Γ** and **L** points visible at smaller volume are found *below* ε_F at V=10.4 $Å^3$/at. Hence, the DMFT calculations show that the topology of the Fermi surface changes under compression. Indeed a comparison of Figs. 3 (a) and (b) shows that hole pockets appears at **Γ** and **L** with decreasing volume, and therefore *hcp* Fe undergoes an *electronic topological transition* [34]under applied pressure. We have checked that the predicted ETT is robust with respect to variations in the strength of the local Coulomb interaction and is not influenced by numerical inaccuracies and stochastic errors; see Sec. 2.4 of Supplementary [16]. The actual ETT takes place at pressures in the range from 40 to 80 GPa for the value of the Coulomb parameter U ranging from 2.9 to 3.9 eV, respectively. It is remarkable that the observed ETT is absent in the LDA calculations (as well as in GGA, see Sec. 2.3 of Supplementary [16]); it appears only upon inclusion of correlation effects.

The effects of ETT on the lattice properties of metals within the one-electron approximation are well understood [35]. The elastic moduli C_{ii} calculated at the condition of constant particle number at the deformation contains the contribution

$$\delta C_{ii} = -\frac{1}{V_0}\sum_{\lambda}\left(\frac{\partial \xi_\lambda}{\partial u_i}\right)^2 \delta(\xi_\lambda), \qquad (1)$$

where $\xi_\lambda = \varepsilon_\lambda - \varepsilon_F$, and ε_λ denotes the single-particle energies. ξ_λ is singular near the ETT, and this singular contribution has the same singularity as $-N(\varepsilon_F)$. This means, in particular, that the peculiarity in the Debye sound velocity is $\Delta V_D \sim -\delta N(E_F)$, where $\delta N(E_F)$ is the change in the density of states (DOS) at the Fermi level due to ETT. In the case of an appearance of a new hole pocket below the critical volume V_{ETT} the change in DOS is $\delta N(E_F) \sim (V_{ETT}-V)^{1/2}$, hence the one-electron theory predicts the existence of square-root-down-shaped peculiarity at the ETT. Our DMFT calculations show that in the case of *hcp*-Fe at moderate compression one should use the Fermi-liquid theory of ETT [36]. In this case many-electron effects cause the singularity of the thermodynamic potential Ω at ETT to be two-sided. Still the leading term is a square root in ΔV_D on one side of the transition, while the peculiarity on the other side of the transition is one power weaker.

The Debye temperature θ_D also has a singularity as $-N(\varepsilon_F)$, and lattice heat capacity at low temperature $T << \theta_D$ has the same singularity as the electron heat capacity. The thermal expansion coefficient proportional to the derivative of θ_D with respect to deformation has a stronger singularity at these temperatures, like $\frac{\partial N(\varepsilon_F)}{\partial \varepsilon_F}$, that is divergent at the point of ETT (e.g., [37]). It is important to stress, however, that the Debye model is qualitatively incorrect in the situation of ETT. Strong anomalies of the phonon spectra in the harmonic approximation occur in a relatively small part of the Brillouin zone near the Γ point and the average phonon frequency over the whole Brillouin zone, which is relevant for thermodynamics at $T \approx \theta_D$, is weaker by a factor of $\varepsilon_F - \varepsilon_c$, where ε_c is the Van Hove singularity energy [38]. However, if we take into account quasiharmonic and anharmonic effects, i.e., the temperature dependence of phonon frequencies due to thermal expansion and phonon-phonon interactions, the

singularities again enhance and become like $N(\varepsilon_F)$ in average phonon frequencies and like $\frac{\partial N(\varepsilon_F)}{\partial \varepsilon_F}$ in the elastic moduli [39].

For *hcp* metals ETTs have been associated with anomalies in the lattice parameter ratio *c/a* in the vicinity of the transition [40–43]. The dependence of lattice constants on the external parameters is less singular than C_{ii} since they are related to the first derivatives of the thermodynamic potential, while C_{ii} are related to the second derivatives. This means that the anomaly in the *c/a* ratio at zero temperature should be hardly visible but at finite (and sufficiently high) temperatures it is proportional to $N(\varepsilon_F)$ via the anomaly of the thermal expansion coefficient, discussed above. The same is true for the second-order Doppler shifts of the Mössbauer spectra related to the heat capacity and, thus, with the average phonon frequencies over the Brillouin zone. Thus, the theory of ETT provides a convincing explanation of the experimentally observed anomalies of the sound velocity, *c/a* ratio and center shift at 40-45 GPa.

To conclude, we observe the electronic isostructural transition of *hcp* Fe and $Fe_{0.9}Ni_{0.1}$ at a pressure of ~40 GPa. The presence of the transition is confirmed by three independent experimental approaches – nuclear inelastic scattering, *c/a* ratio measurement, and Mössbauer center shift determination. The theoretical calculations carried out by means of state-of-the-art *ab initio* methods explain the anomalies in terms of a change of the Fermi surface topology, a so-called electronic topological transition. The existence of the ETT in many-body calculations and its absence in one-electron calculations is a clear signature of correlation effects in the paramagnetic phase of *hcp* Fe. Therefore, advanced approaches beyond the density functional theory are needed to understand the complex physics of this material. Our results also point out to possible importance of many-body effects in other itinerant metallic systems at high-pressure conditions.

We are grateful to Prof. A. Georges for useful discussion. The funding provided by Swedish e-science Research Centre (SeRC), the Swedish Research Council via grant 621-2011-4426, and the Swedish Foundation for Strategic Research (SSF) programs SRL grant 10-0026 and “Multifilms”,as well as financial support from German Science Foundation (DFG) and German Ministry for Education and Research (BMBF) are

acknowledged. Calculations have been performed at the Swedish National Infrastructure for Computing (SNIC). We acknowledge the European Synchrotron Radiation Facility for provision of synchrotron radiation facilities on beamlines ID09a and ID18.

REFERENCES

[1] L. Dubrovinsky, N. Dubrovinskaia, O. Narygina, I. Kantor, A. Kuznetzov, V. B. Prakapenka, L. Vitos, B. Johansson, A. S. Mikhaylushkin, S. I. Simak, and I. A. Abrikosov, Science **316**, 1880 (2007).

[2] K. Shimizu, T. Kimura, S. Furomoto, K. Takeda, K. Kontani, Y. Onuki, and K. Amaya, Nature **412**, 316 (2001).

[3] R. Boehler, Rev. Geophys. **38**, 221 (2000).

[4] A. I. Lichtenstein, M. I. Katsnelson, and G. Kotliar, Phys. Rev. Lett. **87**, 067205 (2001).

[5] J. Kübler, *Theory of Itinerant Electron Magnetism* (Oxford University Press, USA, 2009).

[6] O. N. Mryasov, V. A. Gubanov, and A. I. Liechtenstein, Phys. Rev. B **45**, 12330 (1992).

[7] I. A. Abrikosov, A. E. Kissavos, F. Liot, B. Alling, S. I. Simak, O. Peil, and A. V. Ruban, Phys. Rev. B **76**, 014434 (2007).

[8] I. Leonov, A. Poteryaev, V. Anisimov, and D. Vollhardt, Phys. Rev. Lett. **106**, 106405 (2011).

[9] G. Cort, R. D. Taylor, and J. O. Willis, J. Appl. Phys. **53**, 2064 (1982).

[10] G. Steinle-Neumann, L. Stixrude, and R. E. Cohen, Phys. Rev. B **60**, 791 (1999).

[11] G. Steinle-Neumann, R. E. Cohen, and L. Stixrude, J. Phys.: Condens. Matter **16**, S1109 (2004).

[12] A. B. Papandrew, M. S. Lucas, R. Stevens, I. Halevy, B. Fultz, M. Y. Hu, P. Chow, R. E. Cohen, and M. Somayazulu, Phys. Rev. Lett. **97**, 087202 (2006).

[13] R. Lizárraga, L. Nordström, O. Eriksson, and J. Wills, Phys. Rev. B **78**, 064410 (2008).

[14] V. Thakor, J. B. Staunton, J. Poulter, S. Ostanin, B. Ginatempo, and E. Bruno, Phys. Rev. B **67**, 180405 (2003).

[15] I. I. Mazin, D. A. Papaconstantopoulos, and M. J. Mehl, Phys. Rev. B **65**, 100511 (2002).

[16] see Supplementary information at [URL] for details of experiments and theoretical simulations

[17] A. Georges, G. Kotliar, W. Krauth, and M. J. Rozenberg, Rev. Mod. Phys. **68**, 13 (1996).

[18] G. Kotliar, S. Y. Savrasov, K. Haule, V. S. Oudovenko, O. Parcollet, and C. A. Marianetti, Rev. Mod. Phys. **78**, 865 (2006).

[19] M. Aichhorn, L. Pourovskii, V. Vildosola, M. Ferrero, O. Parcollet, T. Miyake, A. Georges, and S. Biermann, Phys. Rev. B **80**, 085101 (2009).

[20] H. K. Mao, J. Xu, V. V. Struzhkin, J. Shu, R. J. Hemley, W. Sturhahn, M. Y. Hu, E. E. Alp, L. Vocadlo, D. Alfè, G. D. Price, M. J. Gillan, M. Schwoerer-Böhning, D. Häusermann, P. Eng, G. Shen, H. Giefers, R. Lübbers, and G. Wortmann, Science **292**, 914 (2001).

[21] R. Lübbers, H. F. Grünsteudel, A. I. Chumakov, and G. Wortmann, Science **287**, 1250 (2000).

[22] J. C. Crowhurst, A. F. Goncharov, and J. M. Zaug, in *Advances in High-Pressure Technology for Geophysical Applications* (Elsevier, 2005), pp. 3–23.

[23] J. F. Lin, V. V. Struzhkin, W. Sturhahn, E. Huang, J. Zhao, Y. M. Hu, E. E. Alp, H.-K. Mao, N. Boctor, and R. J. Hemley, Geophys. Res. Lett. **30**, (2003).

[24] H.-K. Mao, Y. Wu, L. C. Chen, J. F. Shu, and A. P. Jephcoat, J. Geophys. Res. **95**, 21737 (1990).

[25] L. S. Dubrovinsky, S. K. Saxena, F. Tutti, S. Rekhi, and T. LeBehan, Phys. Rev. Lett. **84**, 1720 (2000).

[26] A. Dewaele, P. Loubeyre, F. Occelli, M. Mezouar, P. I. Dorogokupets, and M. Torrent, Phys. Rev. Lett. **97**, 215504 (2006).

[27] Y. Ma, M. Somayazulu, G. Shen, H. Mao, J. Shu, and R. J. Hemley, Physics of the Earth and Planetary Interiors **143–144**, 455 (2004).

[28] R. Boehler, D. Santamaría-Pérez, D. Errandonea, and M. Mezouar, Journal of Physics: Conference Series **121**, 022018 (2008).

[29] S. Ono, T. Kikegawa, N. Hirao, and K. Mibe, American Mineralogist **95**, 880 (2010).
[30] W. Potzel, M. Steiner, H. Karzel, W. Schiessl, M. Köfferlein, G. M. Kalvius, and P. Blaha, Phys. Rev. Lett. **74**, 1139 (1995).
[31] C. S. Yoo, J. Akella, A. J. Campbell, H. K. Mao, and R. J. Hemley, Science **270**, 1473 (1995).
[32] W. L. Mao, A. J. Campbell, D. L. Heinz, and G. Shen, Physics of the Earth and Planetary Interiors **155**, 146 (2006).
[33] P. Werner, A. Comanac, L. de' Medici, M. Troyer, and A. Millis, Phys. Rev. Lett. **97**, 076405 (2006).
[34] I. M. Lifshitz, Soviet Phys. JETP **11**, 1130 (1960).
[35] M. I. Katsnelson, I. I. Naumov, and A. V. Trefilov, Phase Transitions **49**, 143 (1994).
[36] M. I. Katsnelson and A. V. Trefilov, Phys. Rev. B **61**, 1643 (2000).
[37] P. Souvatzis, O. Eriksson, and M. I. Katsnelson, Phys. Rev. Lett. **99**, 015901 (2007).
[38] V. G. Vaks, M. I. Katsnelson, A. I. Likhtenstein, G. V. Peschanskikh, and A. V. Trefilov, J. Phys.: Condens. Matter **3**, 1409 (1991).
[39] V. G. Vaks and A. V. Trefilov, J. Phys.: Condens. Matter **3**, 1389 (1991).
[40] S. Meenakshi, V. Vijayakumar, B. K. Godwal, and S. K. Sikka, Phys. Rev. B **46**, 14359 (1992).
[41] D. L. Novikov, A. J. Freeman, N. E. Christensen, A. Svane, and C. O. Rodriguez, Phys. Rev. B **56**, 7206 (1997).
[42] V. V. Kechin, Phys. Rev. B **63**, 045119 (2001).
[43] Z. Li and J. S. Tse, Phys. Rev. Lett. **85**, 5130 (2000).

Figure captions:

Figure 1 (color online)

Debye sound velocity V_D as a function of pressure for pure iron (filled black squares, -1-) and $Fe_{0.9}Ni_{0.1}$ alloy (open triangles,-2-). The upper axis shows the density scale. Also shown are literature data on sound velocities obtained with NIS (open circles [20],-4- and half-filled circles [21],-5-), and impulsive stimulated light scattering (ISLS) measurements [22] (circles with crosses, -6-) for pure ε-Fe, as well as NIS data [23] for ε-$Fe_{0.92}Ni_{0.08}$ (blue open squares,-3-). Experimental data presented in the figure show the softening of V_D in a pressure region of 42-52 GPa.

Figure 2

Experimental pressure dependence of (a) *hcp* phase lattice parameter *c/a* ratio and (b) the Mössbauer centre shift based on several experimental datasets for pure iron (red circles) and for $Fe_{0.9}Ni_{0.1}$ alloy (blue circles). The centre shift values are given relative to pure *bcc* iron. Straight grey lines in (a) are guides for the eye.

Figure 3.

The LDA+DMFT ***k***-resolved spectral function *A(**k**,E)* (in V_{at}/eV, where V_{at} is the volume per atom) of *hcp* Fe at volumes of 8.9 Å^3/at (*a*) and 10.4 Å^3/at (*b*) corresponding to pressures of 69 and 15.4 GPa, respectively. The energy zero is taken at the Fermi level. The hole-like bands at the **Γ** and **L** points at volume 8.9 Å^3/at (indicated by the white arrows) are *below* E_F at V=10.4 Å^3/at. The corresponding LDA band structures are shown in *e* and *d*, respectively. In (e) and (f) the corresponding LDA+DMFT Fermi surfaces are shown for the same volumes. The full Fermi surface is plotted on the left-hand side and its cut along the Γ-M direction is displayed in the right-hand side. Changes of the FS topology around the L and Γ points are clearly seen.

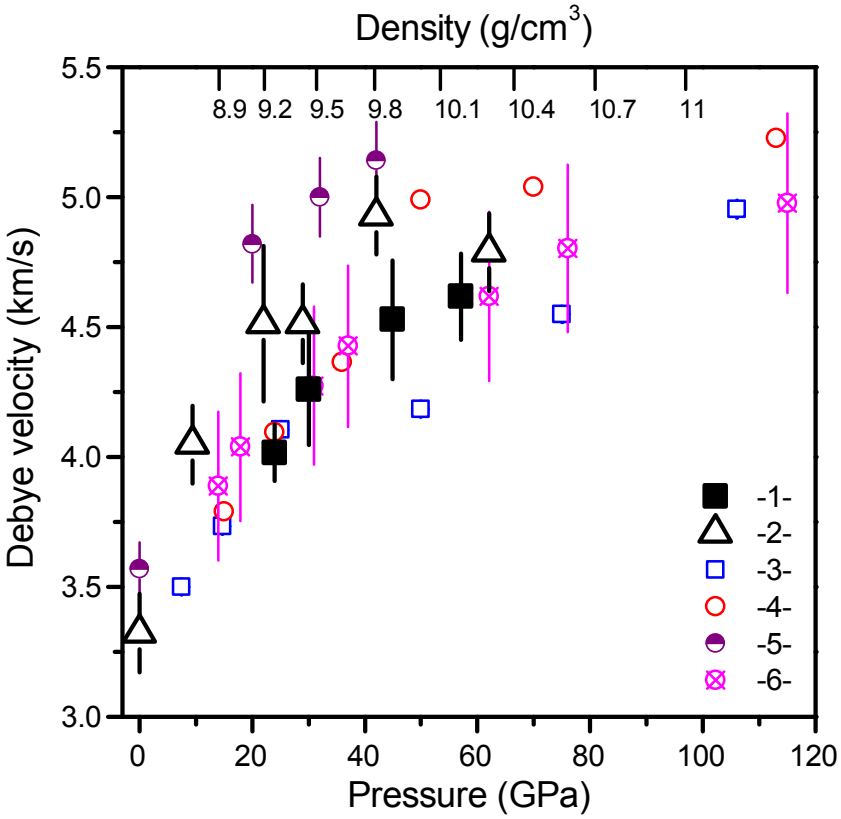

FIG. 1 (color online)

323

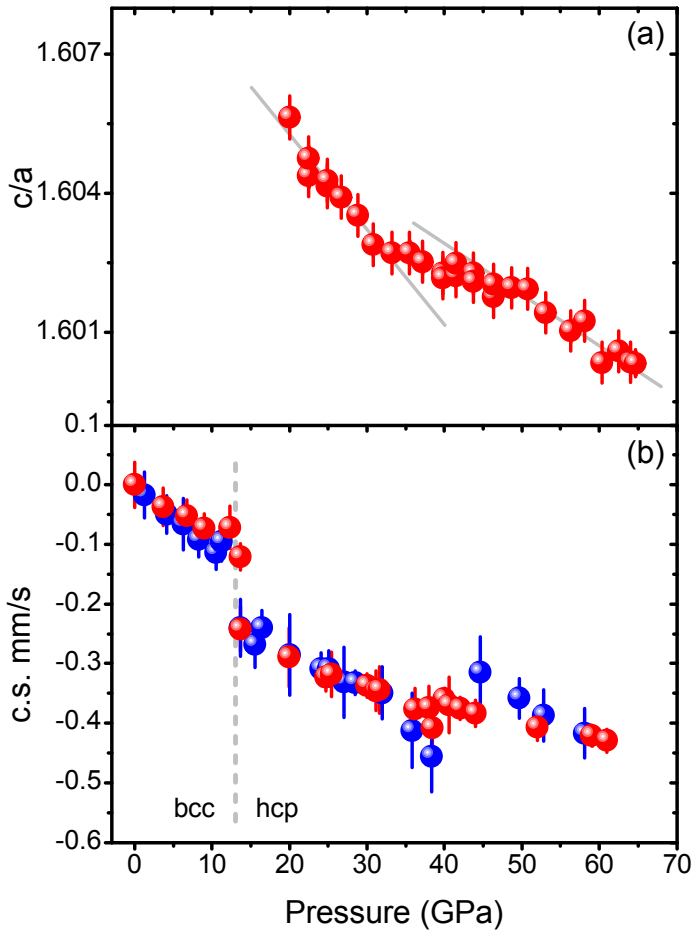

FIG. 2

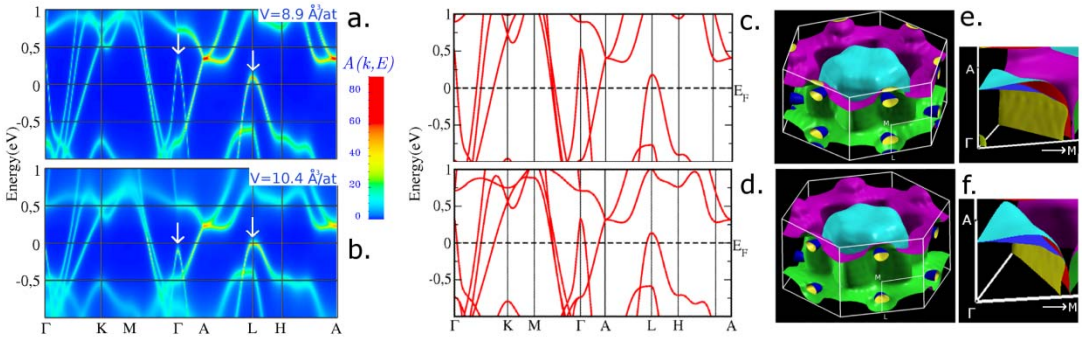

FIG. 3.

324

325